Route to chaos in a hybrid bistable system with delay

J. Y. Gao,* L. M. Narducci, L. S. Schulman,† M. Squicciarini, and J. M. Yuan
Physics Department, Drexel University, Philadelphia, Pennsylvania 19104
(Received 24 June 1983)

A systematic study of the temporal evolution and of the power spectrum of the output intensity produced by a hybrid bistable system with a delay in the feedback loop has shown that self-pulsing and chaotic oscillations are the result of the nonlinear coupling among an infinite number of modes of the linearized system. The main qualitative differences observed both experimentally and in computer simulations between short- and long-delay-time regimes are caused by the emergence of progressively more unstable modes as the delay of the feedback is made larger. The fairly abrupt changes in the temporal patterns, which in earlier numerical studies have been interpreted as periodicity windows are, instead, the result of frequency locking among a large number of modes of the system. From this work we conclude that the short- and long-delay-time regimes do not differ fundamentally from one another, and can easily be described in terms of a common analysis.

The delayed action of the feedback mechanism in a bistable system driven by a constant input field is known to produce periodic or irregular self-pulsing in the output intensity under appropriate conditions.[1,2] Experimental evidence of this effect was first provided with a hybrid electro-optic device in which the delay of the feedback loop was made considerably larger than the inverse bandwidth (response time) of the system.[3] In this case the instability was observed to generate an output train of nearly square pulses, with a period approximately equal to twice the delay time, which progressed into a chaotic structure upon varying the intensity of the external cw field. In these experiments no clear evidence was found for the existence of an infinite sequence of period-doubling bifurcations, although the investigators have reported the unexpected appearance of frequency locking.[3]

Independent experimental tests on a similar type of bistable system have uncovered a very different phenomenology,[4] unfortunately without the benefit of a clear clue for understanding the origin of the observed differences. An important aspect of the experiments discussed in Ref. 4 is that the delay of the feedback loop was comparable in magnitude to the system's response time, thus suggesting that perhaps the nature of the self-pulsing instability and the mechanism for the emergence of chaos might depend in a sensitive way on the length of the delay.

A theoretical analysis of this problem was carried out by Gao *et al.*[5] in an attempt to clarify some aspects of this problem. As anticipated, their computer simulations of the output intensity for long-delay times displayed the characteristic square wave shape reported in Ref. 3. For short delays, however, the situation was considerably more complicated, as one might expect on the basis of the results of Ref. 4. Computer scans corresponding to a fixed value of the (unstable) steady-state output intensity displayed nearly sinusoidal oscillations just beyond the instability threshold; these were followed, for larger delays (but not uniformly for all values of the incident intensity), by what appeared to be bifurcated solutions of the $2P$ and $4P$ period-doubling type, at least judging from the shape of the time-dependent solutions. On the other hand, no evidence again was found in support of the existence of an infinite sequence of period-doubling bifurcations, such as observed, for example, in other models or optical bistability.[6]

To complicate the picture, a very detailed theoretical analysis[7] of the Ikeda model, which in the dispersive limit produces the governing equations of this hybrid device, has proved the existence of period-doubling sequences which are consistent with Feigenbaum's universality conjecture[8] when the delay of the feedback loop becomes infinitely long.

In this paper we report the results of further studies of this problem based on the analysis of the power spectra of the output intensity. As we show below, the spectral analysis,[9] coupled to a precise knowledge of the complex eigenvalues of the linearized problem, and further aided by the corresponding time-dependent output intensity solutions, provides a powerful tool for describing some of the general features of this system. With the help of these tools, we have gained a qualitative understanding of the origin of the periodic and chaotic oscillations and clarified the relation between the short and long delay limits of the bistable model. The system is described by the coupled-delayed equations,

$$x(t)=\tfrac{1}{2}y\{1-\kappa\cos[\theta+V(t)]\}\ , \tag{1.1}$$

$$\frac{dV(t)}{dt}+V(t)=x(t-T)\ , \tag{1.2}$$

where y and $x(t)$ represent the input and output intensity levels and $V(t)$ the feedback voltage; T is the delay time in the feedback loop, θ measures, in units of the half-wave voltage, the fixed bias applied to the electro-optic element, and κ is the modulation depth of the device. Both T and the time variable are scaled to the response time of the hybrid system, and, thus, are dimension-free. The stability of the steady state $[dV/dt=0,\ x(\infty)=V(\infty)]$ is controlled by the transcendental equation

$$S+1-\frac{\kappa}{2}y\sin[\theta+x(\infty)]e^{-TS}=0 \tag{2}$$

as discussed in some detail in Refs. 4 and 5. An important point for the present discussion is that Eq. (2) admits an infinite number of solutions. The real part of each root measures the characteristic (amplification or damping) rate of the corresponding linearized mode, while the imaginary part measures the oscillation frequency. When $\mathrm{Re}S > 0$, the linearized mode, corresponding to the eigenvalue S, is unstable.

A convenient way to survey the distribution of the roots of the secular equation (2) is shown in Figs. 1(a) and 1(b). Figure 1(a) is a representative of all the unstable situations corresponding to a delay time T of the order of unity. The characteristic feature of this range of delay times is the existence of no more than one unstable mode for all values of the input field for which one can observe a self-pulsing output. On the contrary, when T becomes sufficiently large, the real parts of the eigenvalues cluster to such an extent that even a small change in the input field can cause a large number of modes to become unstable all at once.[10] Furthermore, the imaginary parts of the roots approach values that are *odd* multiples of π/T and become nearly commensurate, a circumstance that greatly favors the onset of frequency locking. This feature of the spectrum (i.e., the existence of only the odd multiples of the fundamental frequency) is at the origin of the observed square wave pattern for large delays. Thus, the very different appearance of the periodic self-pulsing outputs observed experimentally in Refs. 3 and 4 is easily traced back to the different structure of the eigenvalue spectrum in the small- and long-delay-time regimes. Surprisingly, as we shall see, the power spectra of the output intensity are not as qualitatively different from each other in the

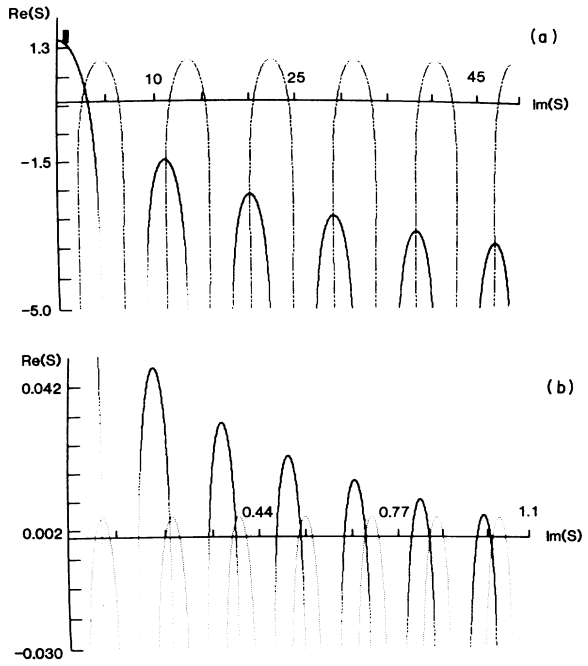

FIG. 1. Graphical display of the complex roots of Eq. (2). Solutions of the secular equation lie at the intercept of the two families of curves. Horizontal and vertical axes label the imaginary and the real parts of the roots, respectively. Thus the points of intercept located above the horizontal axis correspond to unstable modes of the system. Figure (a) has been drawn for $x(\infty)=3.6$ and $T=0.7$. Figure (b) corresponds to $x(\infty)=2.6$ and $T=40$. In all our computer simulations, we have selected $\kappa=0.8$ and $\theta=\pi/2$.

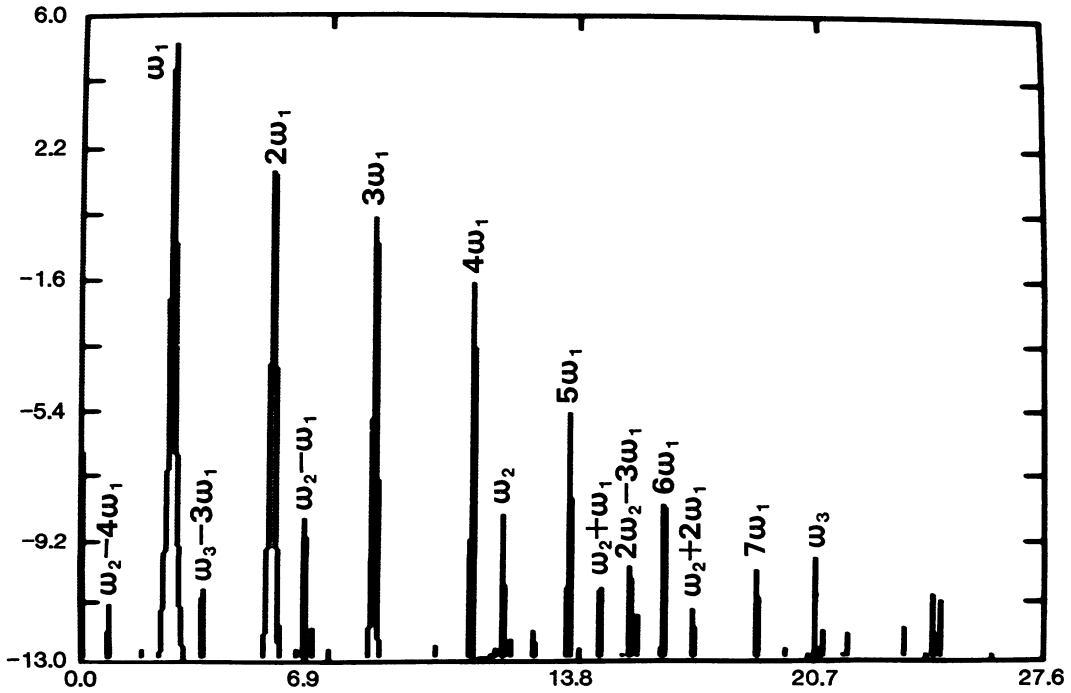

FIG. 2. Power spectrum of the output intensity corresponding to $x(\infty)=3.6$ and $T=0.7$. The horizontal frequency axis is scaled in units of the system bandwidth (same units as used for the calculation of the eigenvalues). Main components of the spectrum are labeled in the figure. The remaining components have also been identified, but have not been labeled for clarity.

two regimes as one might expect.

We now summarize our findings with the help of two typical scans, the first corresponding to a fixed value of the intensity and variable delay times of the order of unity, the second corresponding to a large fixed value of T and variable input intensity. In all cases, the solutions of the time-dependent equations have been obtained by formally integrating Eq. (1.2) and then solving numerically for the time-dependent voltage $V(t)$ from the accumulated knowledge of the previous history of this variable. Several standard and not so standard tricks have been developed to make the calculation as efficient and accurate as possible; in addition, we have carried out all the normal checks to ensure the reliability of the time-dependent solutions.

A typical spectral output corresponding to a periodic signal for $T=0.7$ is shown in Fig. 2. The large and easily recognizable features are of the fundamental frequency and its harmonics. Several other frequency components of the spectrum are rather close to the imaginary parts of the stable eigenvalues of the linearized problem. The small differences are due, almost certainly, to the nonlinear coupling among the linearized modes. By way of illustration, we have listed in Table I a number of eigenvalues and the corresponding frequencies from the calculated power spectrum.[11] The additional smaller spectral features, besides the ones already discussed, are easily interpreted as combination tones of the various components. A few of them have been identified in Fig. 2 (the others which also result from frequency mixing have not been labeled for clarity). Needless to say, the close match of the main spectral lines with the imaginary parts of the linearized eigenvalues offers an extremely convenient way to identify all the essential features of even very complex-looking spectra.

A graphical summary of the above is provided in Figs. 3(a) and 3(b), where the real and imaginary parts of the eigenvalues have been plotted as functions of the delay time T, and where the imaginary parts can be compared directly with the corresponding frequencies calculated from the power spectrum. This behavior is characteristic of all values of the input intensity, and not typical of only the case displayed in this figure. An interesting feature of these results is not only the unexpected small difference between the frequencies of the linearized modes and the corresponding nonlinear spectral components, but also the appearance of frequency looking corresponding to a delay

TABLE I. Real and imaginary parts of the first four eigenvalues of the eigenvalue equation (2) for $x(\infty)=3.6$ and $T=0.7$. The column labeled ω_i lists the position of the appropriate peaks in the power spectrum. The frequencies are measured in units of the system's bandwidth (inverse of the response time).

Real (s)	Imaginary (s)	ω_i
0.335	2.867	2.667
−1.468	11.161	11.518
−2.310	20.102	20.371
−2.838	29.081	29.219

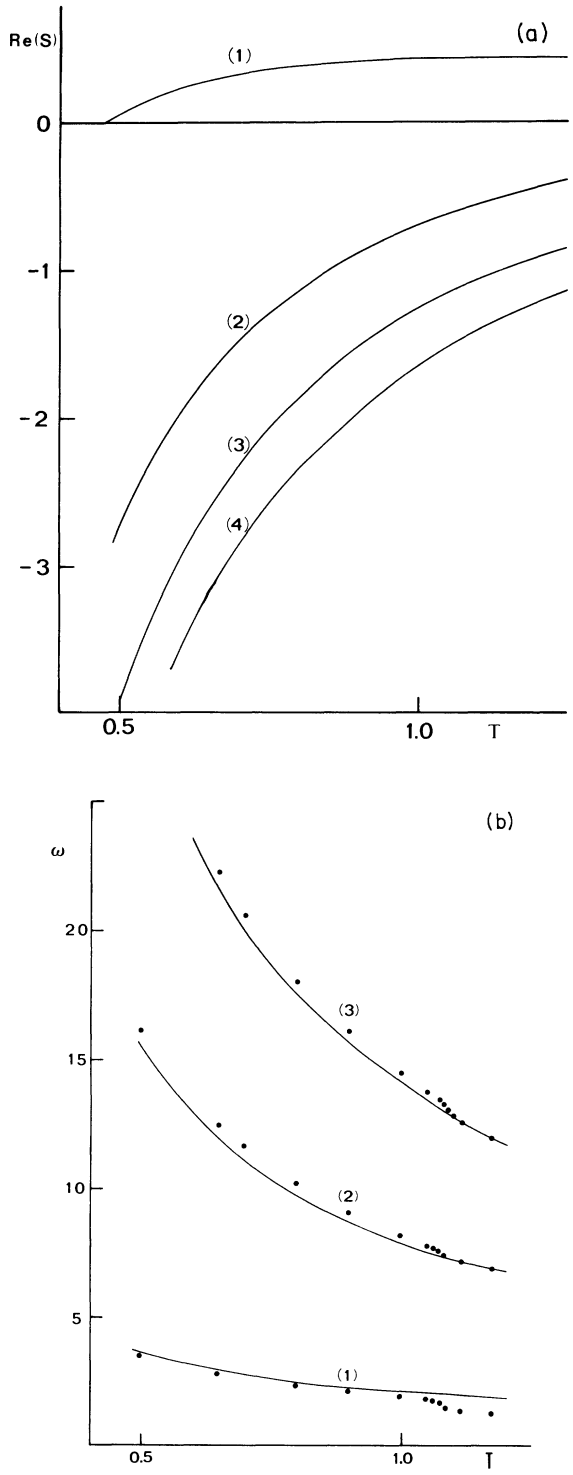

FIG. 3. (a) Dependence of the real parts of the eigenvalues on the delay time T in the small delay range for $x(\infty)=3.6$ Numbers 1–4 label the successive eigenvalues. (b) Imaginary parts of the eigenvalues (solid lines) are plotted as a function of the delay time. Dots identify the location of the appropriate peaks from the power spectra corresponding to $x(\infty)=3.6$. When T becomes approximately 1.07 frequency locking occurs. When $T=0.9$, a subharmonic component is observed in the spectrum. This occurrence has no apparent influence on the behavior of the frequencies plotted in this figure.

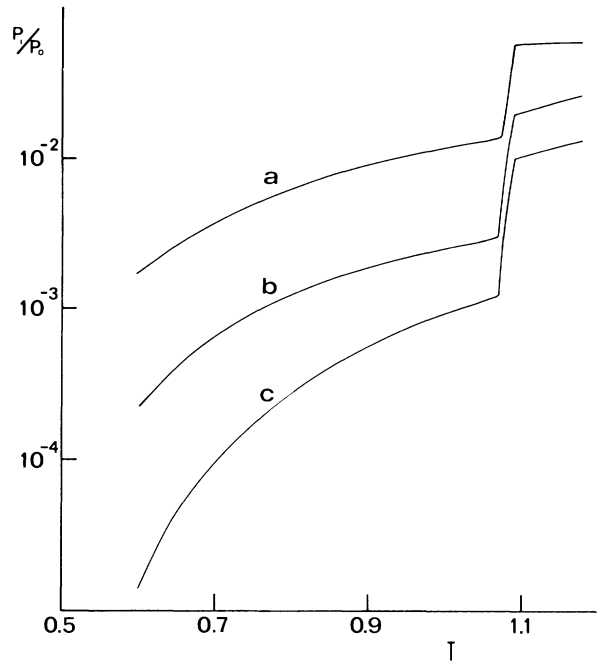

FIG. 4. Ratios of the 2nd (a), 3rd (b), and 4th (c) harmonic powers to that of the fundamental line as functions of the delay time T. Rapid increase in the power ratios corresponds to the occurrence of frequency locking.

T of about 1.07. The occurrence of this phenomenon was reported in Ref. 3 for much larger values of the delay. In our earlier report,[5] we noted the emergence of what seemed to be periodicity windows. This interpretation of the time-dependent solutions was motivated by the appearance of a much more regular structure of the output intensity when T was increased beyond the value 1.07. The power spectrum shows, instead, unambiguously that the spectral lines are commensurate with the fundamental frequency and that the regular structure of the output intensity is the result of frequency locking.

An important additional clue to the dynamical behavior of the system is provided by the ratio of the integrated power of the various peaks to that of the fundamental frequency.[12] The dependence of this ratio on the delay time for a fixed value of the input intensity is shown in Fig. 4. From these data we see that beyond the instability threshold, the integrated power of the harmonic components grows steadily (as expected) but rises very sharply around $T \simeq 1.07$. The power of the spectral peaks corresponding to the stable eigenvalues of the secular equation is very small (typically 6–8 orders of magnitude below the main peak) but it suddenly grows in the neighborhood of $T=1.07$ by about 3–4 orders of magnitude. At this point, all the frequency components of the spectrum are commensurate with the fundamental. At about $T=0.9$, the fundamental frequency undergoes a subharmonic bifurcation which is readily observed both in the time series of the output intensity and in the power spectrum. Its role in the overall picture is not clear, however, aside from it being responsible for a string of combination frequencies at half integral multiples of the fundamental. At

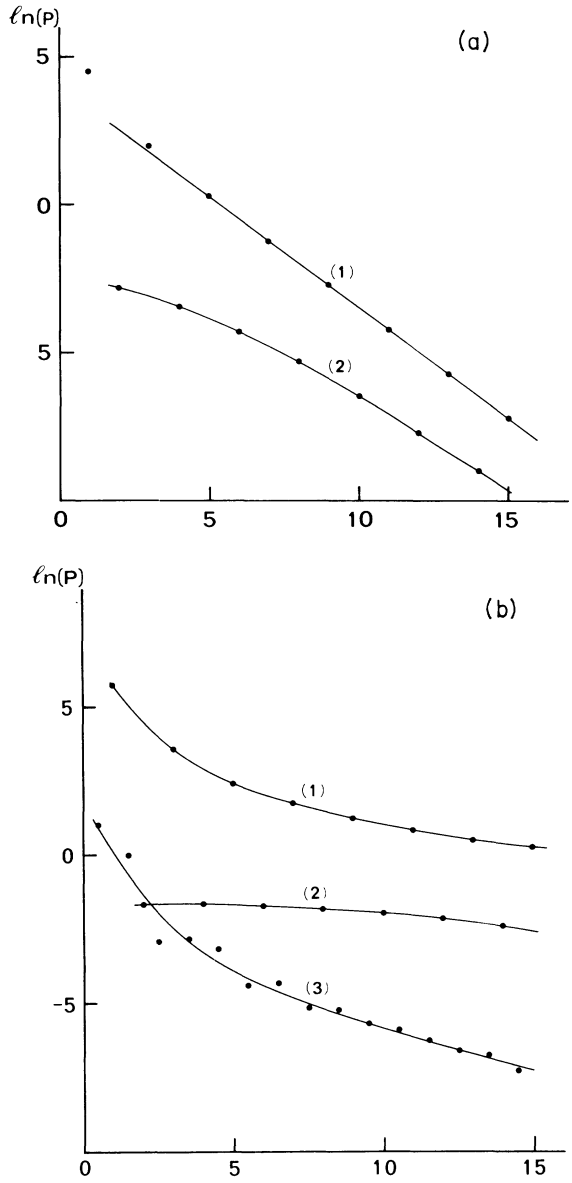

FIG. 5. (a) Logarithm of the integrated spectra power for the fundamental and the next 14 harmonics corresponding to $x(\infty)=2.5$ and $T=40$. The integrated power is calculated in arbitrary units. The horizontal axis labels the order of the harmonics. Two solid lines, 1 and 2, connect the integrated power values of the odd and the even harmonics. (b) Logarithm of the integrated spectral power for the fundamental, the next 14 harmonics and the combination frequencies caused by the presence of the subharmonic frequency $\frac{1}{2}\omega_{\text{fund}}$. Solid lines connect the odd (1) and even (2) harmonics, and (3) the combination frequencies.

about $T=1.2$, apparently, the frequency locking is lost, and the very large number of excited spectral components oscillating out of synchronism, rapidly cause the intensity pattern to acquire a very irregular shape.

For large values of the delay ($T=40$) the picture does not change in a substantial way. The main difference, relative to the short-delay regime, is that even small changes

in the input field cause many linearized modes to become unstable nearly simultaneously. Typical power spectra, calculated for $T=40$ and values of the input field slightly above the self-pushing threshold, show strong locking of all the frequencies, with the odd harmonics dominating the even harmonics by several orders of magnitude [Fig. 5(a)]. For larger values of the incident field, a subharmonic bifurcation is observed [Fig. 5(b)] together with a strong growth of all the spectral components relative to the fundamental. Eventually, as noted in the short-delay case, the frequency locking appears to be lost and the spectrum quickly acquires broad and unresolved features, while the output intensity displays aperiodic and erratic behavior. Here again the transition to chaos is rather abrupt and highly suggestive that the loss of synchronism among the strongly excited components lies at the origin of the observed behavior.

In conclusion, the spectral analysis of the temporal intensity records may have taken some of the mystery away from the origin of the erratic oscillations which have been predicted and observed in this hybrid bistable system. The unstable evolution, for short delays, is dominated at first by the only unstable mode and its harmonics. The stable modes, whose natural frequencies are incommensurate with that of the fundamental, gradually become more important contributors to the system's dynamics, as a result of the nonlinear mode-mode coupling which is enhanced for increasing values of T above the instability threshold [for fixed $x(\infty)$]. Frequency locking characterizes a range of delays where all the infinite modes of the system apparently oscillate in synchronism, and at the end of this range, loss of synchronism results in erratic behavior. For large delays the picture remains qualitatively the same, except that because of the structure of the eigenvalue spectrum (the imaginary parts of the eigenvalues are very nearly commensurate) frequency locking sets in practically at threshold for self-pulsing.

The overall picture that emerges out of our study is somewhat reminiscent of the Landau scenario: Here, also, the linearized dynamics is characterized by an infinite number of frequency components. However, unlike the case proposed by Landau, we see no sharp break of continuity or additional instabilities heralding the increased role played by new spectral features; on the contrary, chaos appears to result merely from the loss of synchronism of the many excited modes.

It may be significant that periodic behavior persists, in our case, even after the emergence of three or even more independent unstable modes. This differs from the Ruelle-Takens scenario where chaos is likely to occur with the appearance of the third instability.

It is difficult to draw a comparison between our results and the ones presented in Ref. 7. Mention should be made of the fact that the imaginary parts of the eigenvalues become exact odd multiples of the fundamental when $T\rightarrow\infty$ and that an infinite number of modes become simultaneously unstable in this limit. These complications have discouraged us from trying to draw any kind of connection at this time between the finite and infinite delay time cases. This, however, appears to be a worthwhile project to pursue.

We are grateful for the assistance of C. A. Pennise with some of the numerical work. This research was partially supported by a grant from the Martin-Marietta Research Laboratory, by the U.S. Army Research Office under Contract No. DAAG29-82-K-0021, and by the donors of the Petroleum Research Fund administered by the American Chemical Society. The support of the Stein Foundation during the stay of L.S.S. at Drexel University and of the Ministry of Education of the People's Republic of China during the stay of J. Y. G. in the U.S. are gratefully acknowledged.

---

*Permanent address: Physics Department, Jilin University, Changchun, People's Republic of China.

†Permanent address: Physics Department, Technion—Israel Institute of Technology, Haifa 32000, Israel.

[1]K. Ikeda, Opt. Commun. 30, 257 (1979); K. Ikeda, H. Daido, and O. Akimoto, Phys. Rev. Lett. 45, 709 (1980).

[2]L. A. Lugiato, V. Benza, and L. M. Narducci, *Proceedings of the 10th International Symposium on Synergetics*, edited by H. Haken (Springer, New York, 1982), and references therein.

[3]H. M. Gibbs, F. A. Hopf, D. L. Kaplan, and R. L. Shoemaker, Phys. Rev. Lett. 46, 474 (1981); F. A. Hopf, D. L. Kaplan, H. M. Gibbs, and R. L. Shoemaker, Phys. Rev. A 25, 2172 (1982).

[4]M. Okada and K. Takizawa, J. Quantum Electron. QE-17, 2135 (1981).

[5]J. Y. Gao, J. M. Yuan, and L. M. Narducci, Opt. Commun. 44, 201 (1983).

[6]L. A. Lugiato, L. M. Narducci, D. K. Bandy, and C. A. Pennise, Opt. Commun. 43, 281 ; L. M. Narducci, D. K. Bandy, C. A. Pennise, and L. A. Lugiato, *ibid.* 44, 207 (1983).

[7]H. J. Carmichael, R. R. Snapp, and W. C. Schieve, Phys. Rev. A 26, 3408 (1982).

[8]M. J. Feigenbaum, J. Stat. Phys. 19, 25 (1978); see also S. Grossmann and S. Thomae, Z. Naturforsch. 32, A 1353 (1977).

[9]The Fast Fourier Transform routine used in this work was provided to us by Professor Jerry Gollub of Haverford College. We are greatly indebted to him for his generous help.

[10]L. A. Lugiato, M. L. Asquini, and L. M. Narducci, Opt. Commun. 41, 450 (1982).

[11]After selection of an appropriate discrimination level to remove the noise, the central frequency of each peak has been calculated by a formula of the type

$$\bar{\omega}=\sum\omega_i S_i \Big/ \sum S_i \ ,$$

the sum being extended to all the points of the discrete spectrum lying above the discrimination level. The identification of the appropriate level was aided by a display of the spectrum which also avoided using the above formula for peaks that were not properly resolved.

[12]The integrated power has been constructed by adding the values of the spectral intensity above the threshold level for every isolated peak.